AJNR

MR Line-Scan Diffusion-Weighted Imaging of Term Neonates with Perinatal Brain Ischemia

Richard L. Robertson, Liat Ben-Sira, Patrick D. Barnes, Robert V. Mulkern, Caroline D. Robson, Stephan E. Maier, Michael J. Rivkin and Adre J. du Plessis

AJNR Am J Neuroradiol 1999, 20 (9) 1658-1670
http://www.ajnr.org/content/20/9/1658

AJNR Am J Neuroradiol 20:1658–1670, October 1999

MR Line-Scan Diffusion-Weighted Imaging of Term Neonates with Perinatal Brain Ischemia

Richard L. Robertson, Liat Ben-Sira, Patrick D. Barnes, Robert V. Mulkern, Caroline D. Robson, Stephan E. Maier, Michael J. Rivkin, and Adre J. du Plessis

BACKGROUND AND PURPOSE: **MR diffusion-weighted imaging provides early demonstration of neonatal brain infarction. The evolution and limitations of diffusion-weighted imaging findings in newborns, however, have not been evaluated. Using line-scan diffusion imaging (LSDI), we investigated perinatal ischemic brain injury.**

METHODS: **Nineteen term newborns (age, 9 hours to 8 days; mean age, 2.6 days) with perinatal brain ischemia were evaluated using LSDI (1520/62.5/1 [TR/TE/excitations]) (*b* maximum = 750 s/mm^2) and T1- and T2-weighted spin-echo (conventional) MR imaging. Follow-up examinations were performed in seven patients and autopsy in one. Apparent diffusion coefficients (ADCs) were measured in deep gray matter, white matter, the cortex, and focal lesions.**

RESULTS: **Based on conventional MR imaging or pathologic findings, patients were divided into two groups. Group 1 (n = 12) had symmetric/diffuse injury consistent with global hypoperfusion. Group 2 (n = 7) had focal/multifocal injury suggesting cerebrovascular occlusion. ADCs were abnormal at initial examination in 10 newborns in group 1 and in all newborns in group 2. The results of LSDI were abnormal before conventional MR imaging was performed in three newborns in group 1. ADCs were maximally decreased between days 1 and 3 in deep gray matter, perirolandic white matter, and focal lesions. Delayed decreases in ADCs were observed in subcortical white matter from days 4 through 10 in three patients in group 1.**

CONCLUSION: **After global hypoperfusion, LSDI showed deep gray matter and perirolandic white matter lesions before conventional MR imaging. LSDI may underestimate the extent of injury, however, possibly because of variations in the compartmentalization of edema, selective vulnerability, and delayed cell death. Differences in LSDI of symmetric/diffuse and focal/multifocal lesions may reflect differences in pathophysiology or timing of the injury. These findings may have implications for acute interventions.**

Despite technological improvements in obstetric and perinatal care, ischemic brain injury remains a major cause of infant morbidity and mortality (1–3). The neurologic sequelae of perinatal brain ischemia include seizures, spasticity, behavioral disturbances, and developmental delay. Neuroprotective strategies, including the early use of pharmacologic agents and induced cerebral hypothermia, may help to decrease the deleterious effects of brain ischemia (3).

Although clinical outcome is the ultimate criterion by which the efficacy of neuroprotective therapies will be judged, neuroimaging likely will play a significant role in documenting the course and extent of the ischemic injury. The utility of MR imaging in evaluating the asphyxiated neonate is well established (4–10). T1- and T2-weighted (conventional) MR sequences, however, are often normal within the first hours after ischemic insult. This early period overlaps with the narrow, finite ''therapeutic window'' during which neuroprotective interventions will most likely be effective. Therefore, the development and application of neuroimaging techniques sensitive to the very early changes of brain ischemia are desirable. Recent studies have documented that diffusion-weighted imaging can show areas of infarction in perinatal brain ischemia before abnormalities are apparent on conventional MR images (7, 11, 12). This suggests that diffusion imaging may be useful in the early detection of perinatal brain ischemia and likely is to become crucial in the effective and safe use of neuroprotective strategies (7, 11, 12). Nevertheless, previous reports have not addressed changes in the pattern

Received February 10, 1999; accepted after revision April 15.

From the Departments of Radiology (R.L.R., L.B.-S., P.D.B., R.V.M., C.D.R.) and Neurology (M.J.R., A.J.d.P.), Children's Hospital Medical Center and Harvard Medical School, and the Department of Radiology (S.E.M.), Brigham and Women's Hospital and Harvard Medical School, Boston, MA.

This investigation was aided by a grant from the Whitaker Foundation.

Address reprint requests to Richard L. Robertson, MD, Department of Radiology, Children's Hospital Medical Center, 300 Longwood Avenue, Boston, MA 02115.

of injury occurring during the first few days of life. In this study, we describe the evolution of diffusion changes in neonates with suspected perinatal brain ischemia and some potential limitations of early diffusion-weighted imaging. To evaluate the diffusion changes occurring in neonatal brain ischemia, we used a robust quantitative diffusion technique, line-scan diffusion imaging (LSDI), which has been shown previously to yield high-quality images in neonates, children, and adults without the use of head restraints, cardiac gating, or specialized hardware (13–17).

Methods

Patients

We reviewed the clinical records, laboratory results, and neuroimaging studies of 19 term neonates (between 38 and 42 weeks postconceptional age) (Table 1) who were referred for MR imaging within the first 8 days of life to evaluate suspected perinatal brain ischemia. In these patients, abnormalities were present on either the initial or follow-up conventional MR images. The initial studies were performed between 9 hours and 8 days of age (mean age, 2.6 days). In seven patients, LSDI was performed between 9 hours and 23 hours after birth (mean = 16 hours). Nine follow-up examinations were performed in seven patients. Pathologic correlation was available in one patient who died 5 hours after the imaging study.

MR Protocol

The imaging protocol included sagittal or axial T1-weighted conventional spin-echo sequences, a T2-weighted fast spin-echo sequence, and LSDI in all patients. All studies were performed on a 1.5-T imaging system (Signa; General Electric Medical Systems, Milwaukee, WI) using a quadrature head coil. The system was equipped with gradient hardware capable of echo-planar imaging.

Patient Sedation

Eight patients underwent MR imaging without sedation. In 11 patients, sedation was obtained using midazolam hydrochloride 0.1 mg/kg, lorazepam 0.1 mg/kg, or chloral hydrate 50 mg/kg p.o. as provided by neonatal intensive care specialists. All patients were monitored with electrocardiography and pulse oximetry. Some patients required assisted ventilation using magnet-compatible devices. There were no sedation failures.

Conventional MR Parameters

Conventional MR imaging was performed using conventional spin-echo sagittal or axial T1-weighted images (600/20/2; field of view, 20 cm; section thickness, 4 mm; gap,1 mm; acquisition matrix, 256 × 192) and fast spin-echo T2-weighted axial images (3200/85/1; field of view, 20 cm; section thickness, 4 mm; gap, 1 mm; acquisition matrix, 256 × 192; echo train length, 8).

LSDI Parameters

The LSDI technique has been described previously (17). LSDI was performed at 10 axial locations (1520/62.5/1; field of view, 20 × 15 cm; effective section thickness, 7 mm; gap, 0 mm; acquisition matrix, 128 × 128 interpolated to 256 × 192) at $b = 5$ s/mm^2 and $b = 750$ s/mm^2 as the maximum b value applied along the three orthogonal directions (15, 17). The total imaging time was 5 minutes 40 seconds. ADC maps and trace images extrapolated to a b value of 1000 s/mm^2 were generated off-line for each of the 10 locations. The trace images were calculated as the cubed root of the product of the three diffusion axes.

Image Review and Analysis

The conventional MR and LSDI images (both trace images and ADC maps) were reviewed separately by two pediatric neuroradiologists blinded to clinical history. Individual diffusion axis images were not evaluated. The results of the MR imaging were classified as normal or abnormal. If abnormal, the location and extent of lesions were described. In the case of disagreement between the two observers, a third neuroradiologist's interpretation served as a tiebreaker. Interobserver variability was measured using the kappa (κ) statistic (18).

ADC calculations were made according to the Stejskal and Tanner equation (19) $S = S_0 e^{-bADC}$, where b is the diffusion-weighting factor, S is the signal intensity for b = maximum, and S_0 is the signal intensity for $b = 5$ s/mm^2. ADC measurements were made in the ventrolateral thalamus, corona radiata, parietal cortex, frontal cortex, frontal white matter, and parietal white matter by using an approximate 1 cm^2 region of interest (ROI) selected from the $b = 5$ s/mm^2 and trace images in all patients. If a focal abnormality was evident on any of the images, either the $b = 5$ s/mm^2 or trace image, the ADC was measured within the center of the lesion and in a corresponding location in the contralateral hemisphere. The ROI used for ADC measurements were drawn and positioned such that the outer margin of the ROI was entirely within the area of the diffusion abnormality when present and avoided CSF. ADC values from images obtained during the first 72 hours of life (n = 15) were analyzed using Student's t test. Statistical significance was considered to be present at the $P < .05$ level.

Results

Obstetric and Neonatal History

The clinical details of the obstetric histories and neonatal events are summarized along with the imaging findings in Table 1. In seven patients, a clearly defined history of perinatal vascular compromise was present, including placental abruption (n = 3), maternal circulatory arrest (n = 1), umbilical cord prolapse with laceration (n = 1), severe fetal-maternal hemorrhage (n = 1), and tight nuchal umbilical cord with no spontaneous respirations (n = 1) (1, 6). Each of three additional patients experienced a prolonged episode of apnea immediately after birth. In one patient, there was meconium aspiration below the vocal cords. In the remaining seven patients, the perinatal history was nonspecific and included seizures in six patients and postnatal depression in one. The remainder of the clinical evaluation in these seven patients failed to show other causes, such as infection or metabolic disease, to account for the perinatal encephalopathy, and all showed focal abnormalities conforming to a vascular distribution on T2-weighted MR images. Therefore, we think that the clinical and imaging findings for these seven patients are explained best by attributing them to occlusive cerebrovascular disease.

TABLE 1: Clinical data and MR findings of 19 neonates with suspected perinatal brain ischemia

Case	Obstetric/Postnatal History	APGAR (1,5,10 min.)	Cord pH	Age	T1WI Findings	T2WI Findings	LSDI Findings
					Group 1, Symmetric/Diffuse Injury		
					Deep structure injury		
1	Placental abruption, sustained fetal bradycardia at 60 beats per minute	2, 4	7.19	13 hours	Normal	Normal	Normal
				5 days	Bilateral putamen hyperintensity	Subtle bilateral posterior putamen hyperintensity	Bilateral posterior putamen decreased ADC
				6 weeks	Bilateral ventrolateral thalamus/putamen hyperintensity	Subtle bilateral ventrolateral thalamus/putamen hyperintensity	Not performed
2	Maternal circulatory arrest due to anaphylactic reaction to penicillin	1, 4, 7	6.60	2 days	Subtle bilateral ventrolateral thalamus/putamen and perirolandic hyperintensity	Subtle bilateral ventrolateral thalamus/putamen and corona radiata hyperintensity	Bilateral thalamic, hippocampal and perirolandic decreased ADC
				7 days	Bilateral thalamic, hippocampal and subcortical perirolandic hyperintensity	Bilateral thalamic, hippocampal and corona radiata hyperintensity	Bilateral thalami, hippocampi, and corona radiata minimally decreased ADC
3	Maternal cocaine use, placental abruption, meconium staining, heart rate <50	1, 1, 2	6.96	7 days	Normal	Bilateral corona radiata mild hyperintensities	Subtle bilateral corona radiata decreased ADC
4	Premature rupture of membranes, no respirations for 5 minutes	3, 5, 6	7.17	8 days	Bilateral ventrolateral thalamus/putamen and subcortical perirolandic hyperintensity	Bilateral ventral thalamic and corona radiata hyperintensity	No diffusion abnormality
					Diffuse injury		
5	Meconium aspiration below the vocal cords, seizures at 10 hours	NA	NA	16 hours	Normal	Normal	Subtle bilateral ventrolateral thalamic decreased ADC
				4 days	Bilateral ventrolateral thalamus/putamen and subcortical perirolandic hyperintensity; parasagittal hypointensity	Bilateral ventrolateral thalamic and parasagittal ''borderzone'' hyperintensity	Bilateral ventrolateral thalamic and parasagittal ''borderzone'' decreased ADC
				10 days	Bilateral ventrolateral thalamus/putamen and subcortical perirolandic hyperintensity; parasagittal hypointensity	Increased bilateral ventrolateral thalamic and parasagittal white matter and gray matter ''borderzone'' hyperintensities	Normalized
6	Placental abruption; no spontaneous respirations; ventilator dependent; seizures	NA	7.03	18 hours	Normal	Normal	Bilateral mesial temporal lobe, thalamus, basal ganglia and corona radiata decreased ADC

TABLE 1: Continued

Case	Obstetric/Postnatal History	APGAR (1,5,10 min.)	Cord pH	Age	T1WI Findings	T2WI Findings	LSDI Findings
7	Antenatal fetal tachycardia, unresponsive at birth, seizures at 18 hours. No additionally clinically observed events	4, 6, 8	NA	2 days	Subtle bilateral periorolandic subcortical hyperintensity	Subtle bilateral thalamic and corona radiata hyperintensity	Bilateral ventral thalamic and corona radiata decreased ADC
				10 days	Bilateral basal ganglia and diffuse subcortical hyperintensity; diffuse white matter hypointensity	Bilateral thalamic and diffuse white matter hyperintensity with loss of frontal cortical ribbon	Increased ADC in lesions which previously had decreased ADC. New bilateral frontal and parietal white matter decreased ADC
8	Laceration of prolapsed umbilical cord requiring emergency C-section, born apneic and asystolic	0, 4, 4	6.96	3 days	Mild putamen/thalamic hyperintensity	Putamen/thalamic hypointensity and frontoparietal white matter hyperintensity and loss of cortical ribbon	Bilateral thalamus/putamen, corona radiata and occipital lobe decreased diffusion.
				7 days	Bilateral basal ganglia and diffuse subcortical hyperintensity; diffuse white matter hypointensity	Increased ventral thalamic/putamen hypointensity; posterior thalamic and diffuse white matter hyperintensity	Heterogeneous bilateral thalamic and marked parietooccipital white matter decreased ADC
9	Decreased fetal movements last 24 hours of pregnancy. Apnea and seizures at 12 hours	3, 7, 9	NA	3 days	Bilateral basal ganglia and diffuse subcortical hyperintensity; diffuse loss of cortical ribbon	Bilateral ''borderzone'' and deep gray matter hyperintensity	Bilateral ''borderzone'' and deep gray matter decreased ADC
10	Fetal-maternal hemorrhage (Hct = 12%), seizures at 6 hours	0, 0, 2	6.95	3 days	Subtle bilateral basal ganglia and corona radiata hyperintensity; loss of cortical ribbon parietooccipital lobes	Subtle bilateral deep gray matter, frontal, and parietooccipital lobe hyperintensity	Bilateral deep gray matter, frontal, and parietooccipital decreased ADC
				Symmetric/deep plus focal injury			
11	Nuchal cord; no spontaneous respirations for 5 min.	4, 6, 8	NA	16 hours	Normal	Subtle Lt. occipital lobe gray and white matter hyperintensity	Lt. occipital lobe gray and white matter and perirolandic decreased ADC
				5 days	Lt. occipital lobe hypointensity; bilateral perirolandic subcortical hyperintensity	Lt. occipital lobe gray and white matter and perirolandic hyperintensity	Lt. occipital lobe gray and white matter and perirolandic decreased ADC
12	Apnea	5, 8	NA	5 days	Bilateral ventrolateral thalamus/putamen and diffuse subcortical hyperintensity	Bilateral thalamic and corona radiata hyperintensity with loss of left parietal cortical ribbon	Bilateral thalamic, corona radiata, and lt. parietal cortex decreased ADC
				Group2, Focal/Multifocal Injury			
13	Decreased fetal movements last 48 hours of pregnancy; lt. arm and leg seizures at 6 hours	8, 9	7.34	9 hours	Rt. parietal hypointensity	Rt. parietal hyperintensity	Rt. parietal decreased ADC
14	Vacuum extraction, seizures	NA	NA	17 hours	Lt. frontoparietal loss of cortical ribbon	Lt. frontoparietal hyperintensity	Lt. frontoparietal decreased ADC

TABLE 1: Continued

Case	Obstetric/Postnatal History	APGAR (1,5,10 min.)	Cord pH	Age	T1WI Findings	T2WI Findings	LSDI Findings
15	Apnea, seizures	8, 9	7.40	23 hours	Lt. frontoparietal hypointensity	Lt. frontoparietal hyperintensity	Lt. frontoparietal markedly decreased ADC
16	Hypoplastic lt. heart, seizures	NA	NA	2 days	Subtle multifocal hypointensities	Multifocal cortical hyperintensities	Multifocal cortical lesions with decreased ADC
17	Rt. sided focal seizures	7, 9	NA	2 days	Lt. occipital and frontal loss of cortical ribbon	Lt. occipital and frontal hyperintensities	Lt. occipital and frontal decreased ADC
				6 days	Lt. occipital and frontal loss of cortical ribbon	Lt. occipital and frontal hyperintensities	Lt. occipital and frontal decreased ADC
18	Decreased fetal movement 2 days before birth. Deep fetal heart rate decelerations, seizures at 8 hours	1, 8	7.33	2 days	Lt. occipital loss of cortical ribbon	Lt. occipital focal cortical and white matter hyperintensity	Lt. occipital focal cortical and white matter decreased ADC
19	Meconium aspiration above cords, perinatal depression	2, 8	7.18	7 days	Rt. posterior temporal hyperintensity	Rt. posterior temporal hyperintensity	Rt. posterior temporal decreased ADC

Note.—T1WI indicates T1-weighted imaging; T2WI indicates T2-weighted imaging; LSDI indicates line scan diffusion imaging; rt.-indicates right; lt. indicates left; ADC indicates apparent diffusion coefficient; NA indicates not available.

Imaging

For the purposes of analysis, we divided the patients into two groups based on the pattern of injury shown by the last conventional MR imaging study available or on the pathologic results (Table 1). In group 1 (n = 12), the infants had a symmetric or diffuse pattern of injury, which did not conform to a specific arterial territory. Two patients in this group also had focal lesions in addition to symmetric deep structural or diffuse injury. In group 2 (n = 7), the injury was focal or multifocal, asymmetric, and conformed to a vascular distribution. There were no cases of periventricular leukomalacia.

Symmetric/Diffuse Injury

Among the patients in group 1, three patterns of injury were evident. In four patients (patients 1–4), lesions involved the deep gray matter and the perirolandic white matter (Fig 1). In six patients (patients 5–10), a diffuse and symmetric pattern of injury was present, involving not only the deep structures but also the cortex and subcortical white matter (Fig 2). In two patients (patients 11 and 12), a mixed pattern of injury was present with focal lesions in addition to deep gray matter and perirolandic white matter or symmetric cerebral hemispheric injury.

Of the 12 patients in group 1, the initial LSDI examination was interpreted as abnormal in 10. In the two neonates with diffuse injury studied within the first 23 hours of life (patients 5 and 6), LSDI showed regions of decreased ADCs, whereas conventional MR imaging findings were interpreted as normal (Fig 3). One infant (patient 4) did not undergo an initial evaluation until day 8 of life, at which time LSDI findings were interpreted as normal. Nevertheless, injury to the deep gray matter structures and periorolandic white matter was evident on the conventional MR images. In one newborn (patient 1) who initially was studied at 13 hours, the LSDI and conventional MR imaging findings were interpreted as normal (Fig 1A–C). In this patient, ADCs measured in the deep gray matter and perirolandic white matter were within 3% of published normal values (20). On follow-up images obtained at day 5, however, these structures were abnormal on both LSDI and conventional MR images (Fig 1D–F). At 6 weeks of life, the conventional MR imaging showed marked T1 shortening and mild T2 prolongation in the posterior putamen and ventrolateral thalamus bilaterally (Fig 1G).

In the three newborns (patients 5, 7, and 8) with diffuse injury who underwent follow-up MR imaging, the initial LSDI findings were interpreted as showing decreased diffusion only in the deep gray matter, the perirolandic white matter, and, to a lesser degree, the cortex (see Fig 2). Nevertheless, in each of these patients, the ADC values measured in the cerebral subcortical white matter (Table 2) were reduced by an average of 24% (range, 14–

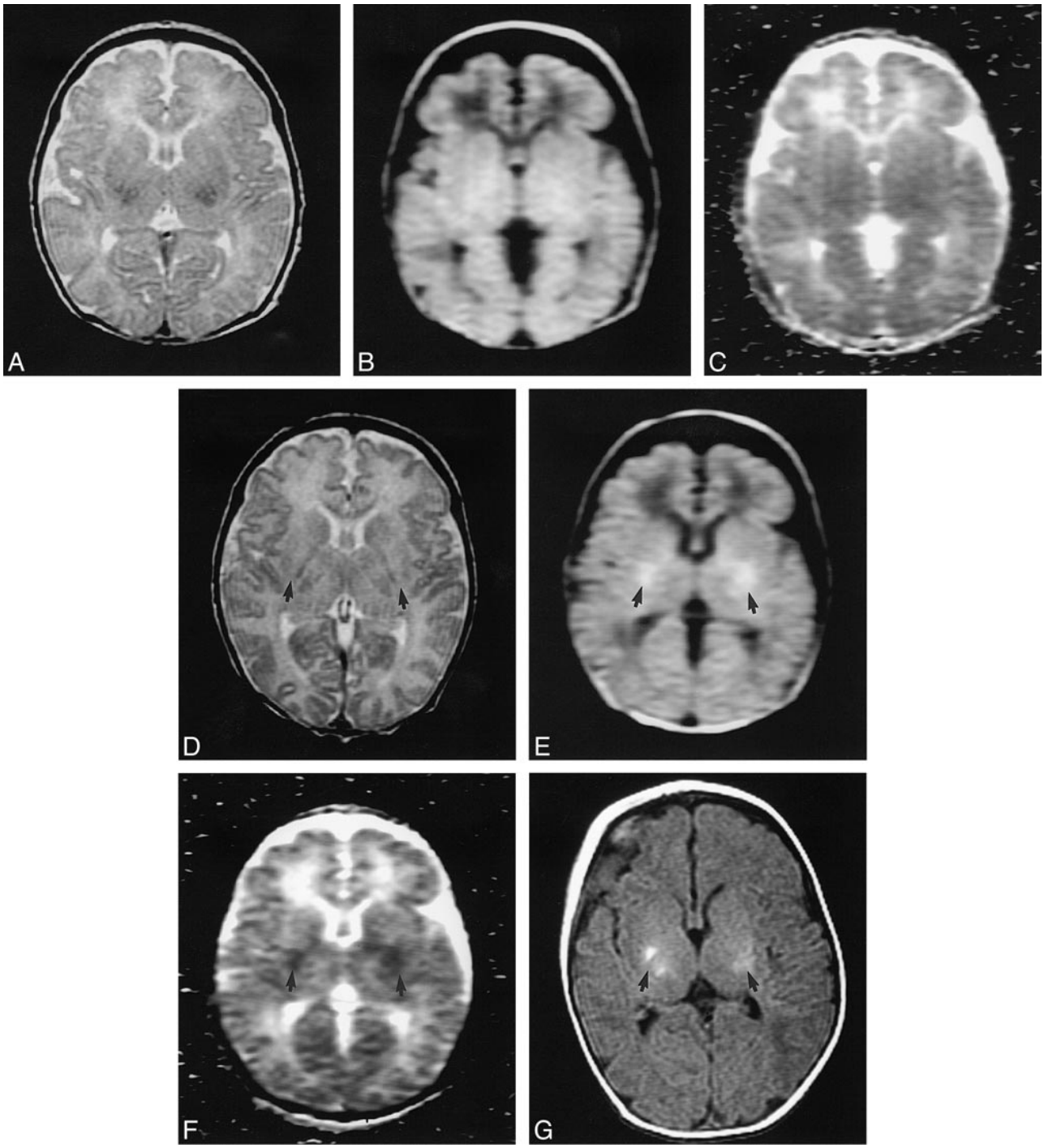

FIG 1. Patient 1. Neonate of estimated 38-week gestational age with placental abruption and bradycardia.

A, Axial T2-weighted fast spin-echo image (3200/85/1), with an echo train length of 8, obtained at 13 hours of life shows no abnormality.

B, Trace LSDI image (1520/62.5/1), with a *b* max of 750 seconds/mm^2, obtained at 13 hours of life shows no abnormality.

C, Corresponding ADC map.

D, Axial T2-weighted fast spin-echo image obtained at 5 days of life shows very subtle hyperintensity in the posterior putamen bilaterally (*arrows*).

E, Trace LSDI image obtained at 5 days of life shows decreased diffusion in corresponding areas (*arrows*).

F, Corresponding ADC map.

G, T1-weighted axial spin-echo image (600/20/2) obtained at 6 weeks of life shows hyperintensity within the posterior putamen and ventrolateral thalamus bilaterally (*arrows*).

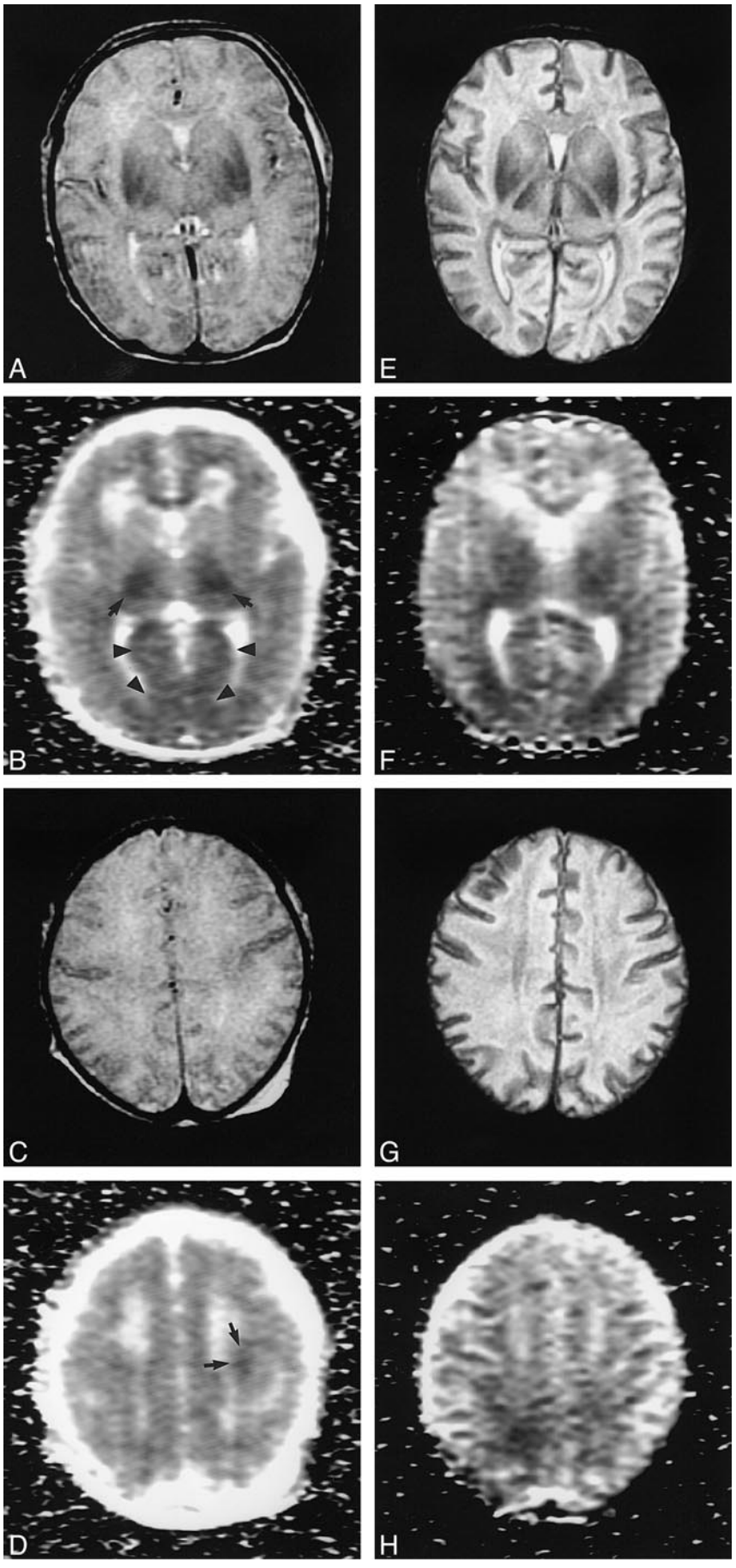

FIG 2. Patient 8. Neonate of estimated 39-week gestational age with a lacerated, prolapsed umbilical cord.

A, Axial T2-weighted fast spin-echo image (3200/85/1), with an echo train length of 8, obtained at 3 days of life at the level of the basal ganglia shows T2 shortening (hypointensity) in the posterior putamen and ventrolateral thalamus bilaterally (compare with Fig 1A). The cortical ribbon is indistinct.

B, ADC map (1520/62.5/1), with a *b* max of 750 s/mm^2, obtained at 3 days of life at a corresponding level shows decreased diffusion (hypointensity) in the ventrolateral thalami (*arrows*) and, to a lesser extent, in the occipital lobe gray matter (*arrowheads*). The hyperintensity of the frontal lobe white matter is due to the high diffusion that is normally present in the white matter of neonates.

C, Axial T2-weighted image obtained at 3 days of life above the lateral ventricles shows loss of the cortical ribbon in the frontal and parietal lobes and mild white matter hyperintensity.

D, ADC map obtained at 3 days of life at the same level shows pathologically decreased diffusion in the left perirolandic white matter (*arrows*). Decreased diffusion was apparent in the right perirolandic white matter at other levels (*not shown*). Note that the white matter of the centrum semiovale apart from the perirolandic white matter does not have decreased diffusion.

E, Axial T2-weighted image obtained at 7 days of life shows marked hypointensity in the posterior putamen/ventrolateral thalami, posterior thalamic hyperintensity, and diffuse white matter hyperintensity.

F, ADC map obtained at 7 days of life at a corresponding location shows heterogeneously decreased ADCs (hypointensity) within the thalami and markedly decreased ADCs throughout the occipital lobe white matter.

G, Axial T2-weighted image obtained at 7 days of life shows marked T2 prolongation within the white matter.

H, ADC map obtained at 7 days of life shows decreased ADCs within the white matter.

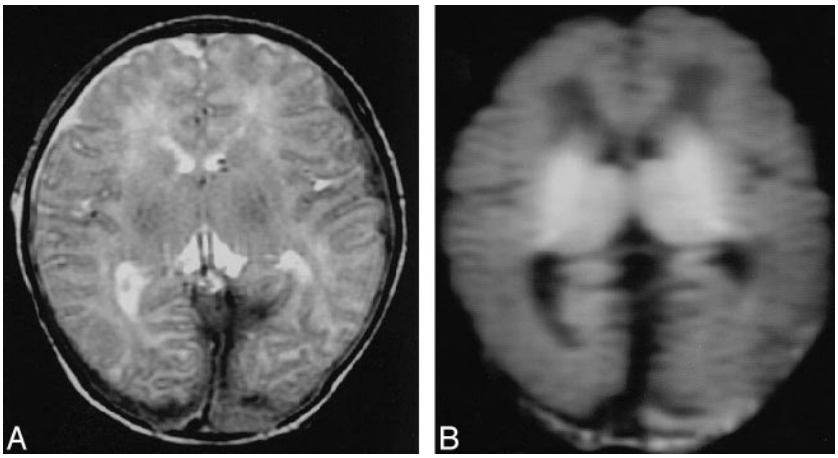

FIG 3. Patient 6. Neonate of estimated 41-week gestational age with placental abruption, no spontaneous respirations, and seizures. Life support was withdrawn at 23 hours of life.

A, Axial T2-weighted fast spin-echo image (3200/85/1), with an echo train length of 8, obtained at 18 hours of life shows no brain abnormality. Small bilateral occipital subdural hematomas are present.

B, Trace LSDI image (1520/62.5/1), with a *b* max of 750 seconds/mm^2, shows decreased diffusion (hyperintensity) bilaterally in the basal ganglia and thalami. Note that the frontal and parietal lobe cortex and white matter appear to have normal diffusion. Pathologic analysis revealed diffuse infarction was present throughout the brain.

TABLE 2: ADC measurements (μm^2/ms) in three neonates with diffuse injury

Case*	Day	Thalami	Parietal Cortex	Frontal Cortex	Perirolandic White Matter	Parietal White Matter	Frontal White Matter
5	1	0.72	0.89	0.96	0.82	1.15	1.22
	4	0.80	0.72	0.84	0.96	0.79	0.85
	10	1.00	1.10	1.05	1.01	1.20	1.32
7	2	0.69	1.0	0.97	0.67	1.29	1.15
	10	0.98	1.1	0.98	1.4	0.48	0.29
8	3	0.49	0.71	0.76	0.53	0.94	0.91
	7	0.77	0.81	0.88	0.96	0.49	0.80

* Refers to the case numbering used in Table 1.

38%) compared with published normal values (20). In these same patients, ADC measurements in the deep gray matter and perirolandic white matter averaged an additional 41% (range, 26–53%) lower than the ADC measurements of the subcortical white matter. The results of the initial conventional MR imaging in one of these newborns (patient 5) studied at 16 hours were normal. In the other two neonates (patients 7 and 8), studied at 2 and 3 days of life, respectively, conventional MR imaging showed diffuse abnormalities. Follow-up MR images of these three patients obtained 3 to 8 days later showed diffuse injury to the deep gray matter, cortex, and subcortical white matter on both the LSDI and conventional MR imaging. Follow-up of these three patients revealed a mean increase of 52% in the ADCs measured in the deep gray matter and perirolandic white matter and a mean decrease of 43% in the ADCs measured in the subcortical white matter (Table 2). ADCs of the cortex on follow-up images were decreased in one patient (patient 5) and increased in the other two (patients 7 and 8). In all three of these patients, no hypoxic-ischemic episodes were observed after the peripartum period.

A fourth neonate (patient 6) with diffuse injury died at 23 hours of life. LSDI at 18 hours of life showed decreased ADCs in the deep gray matter and perirolandic white matter only (see Fig 3). Nevertheless, diffuse early infarctions of the deep gray matter, cortex, and subcortical white matter were evident at autopsy. Both neuronal and oligodendroglial necrosis were present.

Focal/Multifocal Injury

Of the seven neonates in group 2 (patients 13–19), all had decreased ADCs and T2 prolongation involving a vascular territory, as shown by initial imaging. Single lesions were present in five patients, and multiple cortical lesions were identified in two. The injury involved the middle cerebral artery territory in four patients (Fig 4) and the posterior cerebral artery territory in one. In one patient who underwent follow-up imaging, the extent of injury shown on the T2-weighted images was nearly identical to that of the area of involvement on the initial LSDI study.

Image Analysis

Interobserver agreement, as measured by the statistic kappa (κ), was high for both LSDI ($\kappa = 1.0$) and conventional MR imaging ($\kappa = .74$). In the patients in group 1, measured ADCs were maximally decreased in the deep gray matter and perirolandic white matter as shown by studies performed between days 1 and 3. Delayed decreases in ADC values in the frontal and parietal lobes were observed in three patients with diffuse injury.

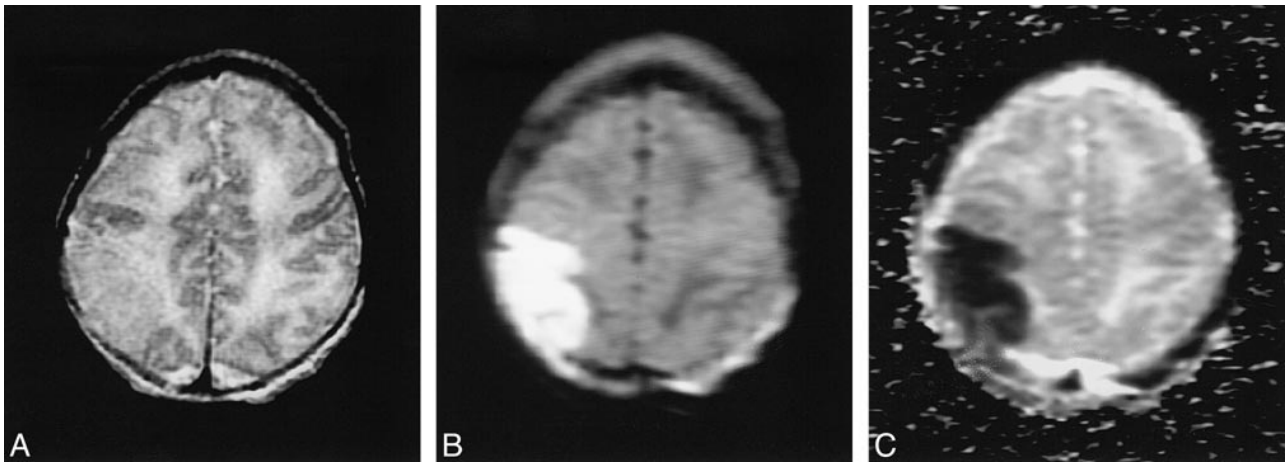

FIG 4. Patient 13. Neonate of estimated 38-week gestational age with decreased fetal movements during the last 48 hours of pregnancy and left arm and leg seizures at 6 hours of life.

A, Axial T2-weighted fast spin-echo image (3200/85/1), with an echo train length of 8, obtained at 9 hours of life shows focal loss of the right parietal cortical ribbon.

B, Trace LSDI image (1520/62.5/1), with a *b* max of 750 seconds/mm^2, shows markedly decreased diffusion (hyperintensity) in a corresponding location.

C, ADC map shows markedly decreased diffusion (hypointensity) within the lesion.

TABLE 3: Mean and standard deviation of ADC measurements (μm^2/ms) in neonates imaged during the first 72 hours with symmetric/diffuse injury (Group 1) versus focal/multifocal injury (Group 2)

Location	Group 1 (symmetric/ diffuse)	Group 2 (focal/ multifocal)	*P* Value
Thalami	0.77 ± 0.20	1.05 ± 0.04	0.005
Parietal Cortex	0.99 ± 0.12	1.15 ± 0.05	0.01
Frontal Cortex	1.02 ± 0.14	1.12 ± 0.03	0.09
Perirolandic White Matter	0.83 ± 0.20	1.16 ± 0.16	0.005
Parietal White Matter	1.17 ± 0.28	1.42 ± 0.15	0.06
Frontal White Matter	1.19 ± 0.28	1.43 ± 0.15	0.09

In the patients with focal lesions, ADCs were maximally decreased on LSDI performed on day 1 or 2. In all seven patients who underwent follow-up imaging between 5 days and 6 weeks of life (median, 7 days), all regions that had decreased diffusion on the initial study had developed signal intensity changes on the conventional MR images.

Statistical analysis was conducted using Student's *t* test comparing ADC measurements obtained from the nine patients in group 1 and the six patients in group 2 who underwent imaging within the first 72 hours of life (Table 3). This analysis showed significantly lower ADCs in the thalami ($P = .005$), perirolandic white matter ($P = .005$), and parietal cortex ($P = .01$) and a trend toward lower ADCs in the parietal white matter ($P = .06$), frontal white matter ($P = .09$), and frontal cortex ($P = .09$) in the neonates with diffuse injury.

Discussion

Diffusion-weighted MR imaging has become an important technique for the evaluation of acute brain infarction (7, 11, 12, 15, 21–29). Studies in both adults and children have focused on the ability of diffusion-weighted imaging to depict acute infarction earlier than T1- and T2-weighted (conventional) MR sequences (7, 11, 12, 21–24). The use of diffusion-weighted imaging in neonates with suspected brain ischemia has been reported (7, 11, 12). The details of evolutionary changes in diffusion imaging during the first few days of life, however, have not been addressed nor have the potential limitations of diffusion imaging in neonates.

Technique Rationale

The development of brain MR protocols in neonates with hypoxic-ischemic injury must take into account a variety of factors. These include the potentially unstable condition of the affected newborn, the small volume and high water content of the neonatal brain, the relatively high ADCs, and the pathophysiology of perinatal brain ischemia. Our neonatal MR protocol was designed to maximize the information content and reliability of the data obtained while minimizing the overall imaging time.

Transportation to the MR suite and sedation of the infants in our study was provided by neonatal intensive care specialists and transport team. All patients were monitored with electrocardiography and pulse oximetry. Assisted mechanical ventilation using magnet-compatible devices was required for some patients.

Our use of T2-weighted fast spin-echo imaging rather than dual-echo conventional spin-echo imaging is based on a previously published systematic comparison of the two imaging techniques in pediatric patients (30). Although proton density–weighted conventional spin-echo images have been

reported to have greater sensitivity than T1-weighted or second-echo T2-weighted conventional spin-echo images (31), our experience has been that the long imaging times required with conventional spin-echo imaging result in a greater number of nondiagnostic examinations because of patient motion. It also has been our experience that the fast spin-echo proton density–weighted images do not show more consistently the early findings of hypoxic-ischemic brain injury compared with the T2-weighted fast spin-echo or T1-weighted conventional spin-echo sequences. Therefore, proton density–weighted imaging was not part of our protocol.

Because diffusion is an inherent tissue property, the diffusion alterations that are observed in association with perinatal ischemic brain injury should be independent of the technique used to measure them. Our choice of LSDI over ''faster'' echo-planar diffusion imaging was based on a previously published comparison of the two techniques (32). In this investigation, LSDI was found to provide more robust diffusion imaging with a significantly higher signal-to-noise ratio and fewer artifacts related to geometric distortion and magnetic susceptibility effects than echo-planar diffusion imaging (32).

A maximum *b* value of 750 s/mm^2, which is lower than that typically used in adults, was used in our study. The decision to use this maximum *b* value was based on our experience that because of the relatively high ADCs of neonatal brain, the use of higher *b* values results in lower quality images because of a significantly reduced signal-to-noise ratio. To increase the apparent diffusion weighting in the ADC maps and trace images without introducing signal loss, we extrapolated the *b* value to 1000 s/mm^2. This postprocessing algorithm is based on previous work (33), which has shown diffusion to be linear over the range of these *b* values. Therefore, the use of only two *b* values in ADC determination is valid. Using additional *b* values would have increased the overall imaging time without significantly improving the precision of the ADC measurements.

Ideally, perfusion imaging should be obtained in newborns with suspected brain ischemia. However, because of the small volume of IV-administered contrast material that can be used and the difficulties in securing adequate IV access for bolus injections, perfusion studies requiring rapid IV administration of contrast material in neonates are typically very poor. Perfusion imaging techniques that do not require IV injection of contrast material, such as the flow-sensitive alternating inversion-recovery technique, provide another option for evaluating cerebral hemodynamics, but have yet to be tested in newborns (34).

Pathophysiology and Imaging

Considering that hypoxic-ischemic reperfusion injury is an evolving and progressive process, temporal and regional differences in the onset of abnormal diffusion might be predicted (1–3). In cases of hypoxic-ischemic reperfusion injury, injury begins with energy failure consequent to acute asphyxia and continues after resuscitation as a number of metabolic derangements are intensified by the reintroduction of oxygen to the affected tissues (3, 35). Vascular endothelial damage caused by hypoxic-ischemic reperfusion injury also promotes leukocyte platelet-mediated vascular occlusion and sustained microvascular constriction, exacerbating the initial ischemic injury (3, 36).

Among the group of infants who sustained global brain injury, LSDI showed ischemic lesions after global hypoperfusion earlier than did conventional T1- and T2-weighted MR imaging (patients 5 and 6). This result is consistent with those of previous reports of diffusion imaging in perinatal brain ischemia (7, 11, 12). In one neonate (patient 4) with suspected perinatal ischemia, LSDI was normal, but conventional MR imaging showed injury to the deep gray matter and perirolandic white matter. This neonate was not studied until 8 days of life, and the ''normal'' results of the LSDI examination may be due to the normalization of ADC values in subacute infarction that has been described previously (24).

A potentially important result of our study was that the initial LSDI performed within the first 72 hours of life (range, 13–72 hours) underestimated the ultimate extent of symmetric/diffuse ischemic injury as shown by follow-up imaging or pathologic study in five patients (patients 1 and 5–8) (Figs 1–3). It seems likely that several factors may be responsible for this underestimation, including variability in the compartmentalization of water after brain ischemia, selective vulnerability, regional delays in the onset of cell death, and timing of the imaging examination.

One factor contributing to the evolution of diffusion abnormalities in hypoxic-ischemic reperfusion injury is temporal variation in the compartmentalization between intracellular and extracellular brain water. Acute infarction is characterized by decreased diffusion. Intracellular (cytotoxic) edema is generally regarded as the most likely cause of this characteristic, although other theories also have been advanced (21, 23, 37–39). It has been shown in neonatal rats subjected to hypoxic-ischemic reperfusion injury that a decrease in extracellular volume fraction occurs within minutes of the onset of ischemia, consistent with cellular swelling (cytotoxic edema) (40). In addition, a number of metabolic processes are initiated during the ischemic episode that predispose the vascular endothelium to injury with reperfusion (3). Reperfusion is often hyperemic, and the damage to the endothelium allows extravasation of fluid and cells into the parenchyma (35). Vasogenic edema begins to occur within the first 24 hours, is maximal at 3 days, and then declines (35). A standard interpretation of the measured ADC is that it represents a weighted av-

erage of the relative volume fractions of intracellular and extracellular water (41). An increase in extracellular volume occurring with reperfusion, therefore, may lead to an overall increase in tissue ADCs even though cellular swelling is ongoing. Considering the relatively large extracellular water fraction of the neonatal brain (42), the presence of vasogenic edema would be expected to have a significant impact on the ADCs of a specified volume of tissue. A decline in ADC values then would be anticipated as the vasogenic edema subsides. This reduction in ADCs accompanying early subacute infarction is followed in late subacute and chronic infarctions by a normalization or increase in ADC values that may be due to cellular shrinkage accompanying the resolution of intracellular edema.

Neonatal animal models of early hypoxic-ischemic reperfusion injury have exhibited a biphasic pattern of diffusion abnormalities that parallels the changes in extent and compartmentalization of brain water (43, 44). In neonatal rats, an initial reduction in ADCs occurs within minutes of the onset of ischemia in the cortical gray matter, white matter, and basal ganglia (40, 43, 44). The decrease in ADCs persists for up to 5 hours after the insult (43, 44). ''Normalization'' of ADCs then occurs during the next 1 to 2 days, followed by a gradual decline (43, 44). The delayed decrease in ADCs observed in the subcortical white matter in patients with diffuse injury in our study therefore may be due in part to a delayed shift of water from the extracellular space to the intracellular space, resolution of extracellular edema, alterations in the permeability of the cell membrane to water, or increased restriction of the diffusion of intracellular water (35, 45, 46).

Recently, the biexponential behavior of water diffusion in the adult human brain was described using multiple *b* factors over a wider range than is generally sampled clinically (33). One possible explanation for this biexponential behavior is that there are differences in the diffusion coefficients of extracellular water versus intracellular water. If this is the case, then sampling multiple *b* factors up to 5000 s/mm^2 might allow the identification of the relative contributions of extracellular and intracellular edema, possibly improving the delineation of the extent of injury during the reperfusion phase.

Another factor influencing early diffusion findings is selective vulnerability (1–3, 6). Areas of the brain that have high-energy requirements, that are actively myelinating, or that contain high concentrations of excitatory neurotransmitters (eg, glutamate) are known to be especially vulnerable to profound hypoxia-ischemia (1, 6). In term neonates, these structures include the brain stem, hippocampi, basal ganglia, thalami, and perirolandic white matter (1, 6, 47). Other regions of the brain, including the subcortical white matter and border zone territories, are more vulnerable to prolonged partial or prolonged profound hypoxic-ischemic insults (6). The presence of markedly decreased diffusion in the deep gray matter structures and perirolandic white matter in patients with diffuse injury is likely related to the vulnerability of these structures to profound hypoxia-ischemia with the rapid development of neuronal and oligodendroglial cellular swelling and cell death.

A final factor contributing to the evolution of diffusion abnormalities in hypoxic-ischemic reperfusion injury is regional variation in the progression to cell death. Although cellular swelling, axonal injury, and cell death may occur rapidly in some regions of the brain, these processes may be delayed in areas that have lower metabolic demands. The existence of delayed neuronal and oligodendroglial cell death due to apoptosis after hypoxia-ischemia has been documented in the frontotemporal cortex and hippocampus of neonatal rats (48). In another study of hypoxia-ischemia in neonatal rats, a late decline in ADCs was partially attributable to the delayed onset of glial swelling (43). Late glial swelling may account for the striking reductions in ADCs of the subcortical white matter observed in patients (eg, patients 5, 7, and 8) with diffuse injury shown on follow-up images at days 4 to 10 of life. If the delayed decreases in ADCs shown in these patients are caused by neuronal or oligodendroglial apoptosis, this may provide an especially important therapeutic window for the use of neuroprotective agents (49).

Based on the possible contributions of temporal variation in the compartmentalization of brain water, selective vulnerability, and delayed cell death, it is apparent that the pattern of injury on diffusion-weighted images is greatly dependent on the timing of the examination relative to the hypoxic-ischemic insult (35, 43, 44). Although none of the patients in our study underwent imaging during the first few hours after the ischemic event, it is possible that very early imaging immediately after reperfusion would more fully show the extent of injury. However, the reversibility of early post-ischemic diffusion abnormalities has been shown experimentally in neonatal rats; therefore, even very early imaging may not reflect the ultimate distribution of injury (44). Recognition that injury may be obscured on diffusion images obtained during the reperfusion phase of hypoxic-ischemic reperfusion injury is extremely important if this technique is to be used to assess neuroprotective interventions.

A potential factor influencing the qualitative interpretation of early diffusion imaging is that a generalized decrease in brain ADCs after global hypoperfusion may be overlooked in the face of more marked decreases in ADCs in the deep gray matter and perirolandic white matter. This factor may have played a minor role in the interpretation of diffusion imaging in the first 72 hours in patients of group 1 in our study. In these patients, there was a significant reduction in ADCs in the thalami ($P = .005$) and perirolandic white matter ($P = .005$) but only a trend toward lower ADCs in the parietal lobe white matter and frontal lobe white matter

when compared with the corresponding but ''uninvolved'' brain regions in neonates with focal injury. In neonates undergoing imaging beyond the first day after insult, this potential pitfall in the interpretation of the diffusion imaging findings may be obviated by inspection of the conventional MR sequences, which typically show abnormal results by 24 to 48 hours (6, 7, 11).

In contrast to the neonates with symmetric/diffuse injury who underwent imaging during the first 24 hours of life, all three infants who had focal injury manifested decreased diffusion on LSDI images during the first day of life, with the earliest examination performed at 9 hours (Fig 4). Differences in the diffusion imaging features of symmetric/diffuse versus focal/multifocal insults have not been previously reported in neonates (7, 11, 12). Precise dating of ischemic brain injury in neonates is often difficult. Although the neonates in our study with focal injury are likely to have suffered perinatal injury, it is not possible to exclude prenatal injury. The presence of T2 prolongation on images obtained as early as 9 hours after birth (patient 13) suggests that at least some of these lesions may have occurred during the prenatal period. However, it is also possible that the imaging differences of focal/multifocal injury and symmetrical/diffuse injury result from pathophysiologic differences.

The pathogenesis of focal or multifocal cerebral infarction is varied and includes vascular maldevelopment, vasospasm, vascular distortion, emboli, and in situ thrombus formation (1, 2). Emboli may originate from the placenta, involuting fetal vessels, indwelling catheters, or within the heart. Thrombus formation may occur secondarily to meningitis, parturitional trauma, hypercoagulable states, or hypoxia-ischemia.

In global hypoperfusion, ischemia is typically incomplete and transient. With vascular occlusion, particularly arterial occlusion, ischemia is likely to be more complete. In addition, reperfusion after arterial occlusion cannot occur until the obstruction is relieved by distal clot migration, collateral development, or vessel recanalization. Postocclusive reperfusion, therefore, is likely delayed in most instances compared with global hypoperfusion. Consequently, there may be a relative absence of vasogenic edema during the early hours after vascular occlusion contributing to the ability of diffusion-weighted imaging to show focal, or multifocal, injury at times when the lesions of diffuse injury are inconspicuous.

Conclusion

Neonates with brain ischemia may develop either symmetric/diffuse injury or focal/multifocal injury. LSDI tends to show ischemic lesions of the deep gray matter and perirolandic white matter earlier than does conventional MR imaging in term neonates, but LSDI findings obtained during the reperfusion phase may be negative or may underestimate the extent of injury in global hypoperfusion. Global hypoperfusion produces an evolving pattern of abnormal diffusion during the first week of life, which likely reflects temporal variations in the compartmentalization of edema, selective vulnerability, and delayed cell death. For our patients with focal/multifocal ischemic brain injury, abnormalities were present on both the conventional MR and LSDI images obtained during the initial examination of all patients, including the patient who underwent imaging at 9 hours of life. Differences in the timing of injury or pathophysiology may provide the basis for differences in the early diffusion-weighted imaging of symmetric/diffuse versus focal/multifocal ischemic brain injury. The results of our findings emphasize the need for prospective studies of very early changes after hypoxia-ischemia if diffusion-weighted imaging is to be used as a means of assessing neuroprotective therapy.

References

1. Volpe JJ. ***Neurology of the Newborn.*** Philadelphia: W.B. Saunders Company;1995:211–372
2. Rivkin MJ. **Hypoxic-ischemic brain injury in the term newborn. Neuropathology, clinical aspects, and neuroimaging.** *Clin Perinatol* 1997;24:607–625
3. du Plessis AJ, Johnston MV. **Hypoxic-ischemic brain injury in the newborn. Cellular mechanisms and potential strategies for neuroprotection.** *Clin Perinatol* 1997;24:627–654
4. Barkovich AJ, Truwit CL. **MR of perinatal asphyxia. Correlation of gestational age with pattern of damage.** *AJNR Am J Neuroradiol* 1990;11:1087–1096
5. Barkovich AJ. **MR and CT evaluation of profound neonatal and infantile asphyxia.** *AJNR Am J Neuroradiol* 1992;13:959–972
6. Barkovich AJ, Westmark K, Partridge C, et al. **Perinatal asphyxia. MR findings in the first 10 days.** *AJNR Am J Neuroradiol* 1995;16:427–438
7. Cowan FM, Pennock JM, Hanrahan JD, et al. **Early detection of cerebral infarction and hypoxic ischemic encephalopathy in neonates using diffusion-weighted magnetic resonance imaging.** *Neuropediatrics* 1994;25:172–175
8. Kuenzle C, Baenziger O, Martin E, et al. **Prognostic value of early MR imaging in term infants with severe perinatal asphyxia.** *Neuropediatrics* 1994;25:191–200
9. Ordidge R, Thornton J, Clemence M, et al. **NMR studies of hypoxic-ischaemic injury in neonatal brain using imaging and spectroscopy.** *Adv Exp Med Biol* 1997;428:539–544
10. Aida N, Nishimura G, Hachiya Y, et al. **MR imaging of perinatal brain damage. Comparison of clinical outcome with initial and follow-up MR findings.** *AJNR Am J Neuroradiol* 1998;19:1909–1921
11. Johnson AJ, Lee BCP, Lin W. **Echoplanar diffusion-weighted imaging in neonates and infants with suspected hypoxic-ischemic injury. Correlation with patient outcome.** *AJR Am J Radiol* 1999;172:219–226
12. Mercuri E, Cowan F, Rutherford M, et al. **Ischaemic and haemorrhagic brain lesions in newborns with seizures and normal Apgar scores.** *Arch Dis Child Fetal Neonatal Ed* 1995;73:67–74
13. Robertson RL, Maier SE, Robson CD, et al. **Line scan diffusion MR imaging of the brain in children.** *AJNR Am J Neuroradiol* 1999;20:419–426
14. Schwartz RB, Mulkern RV, Gubdjartsson H, et al. **Diffusion-weighted MR imaging in hypertensive encephalopathy. Clues to pathogenesis.** *AJNR Am J Neuroradiol* 1998;19:859–862
15. Maier SE, Gubdjartsson H, Patz S, et al. **Line scan diffusion imaging. Characterization in healthy subjects and stroke patients.** *AJR Am J Roentgenol* 1998;171:85–93
16. Huppi PS, Maier SE, Peled S, et al. **Microstructural development of human newborn cerebral white matter assessed in vivo by diffusion tensor magnetic resonance imaging.** *Pediatr Res* 1998;44:584–590

17. Gudbjartsson H, Maier SE, Mulkern RV, et al. **Line scan diffusion imaging.** *Magn Reson Med* 1996;;36:509–519
18. Ker M. **Issues in the use of kappa.** *Invest Radiol* 1991;26:78–83
19. Stejskal EJT. **Spin diffusion measurements. Spin echoes in the presence of a time-dependent field gradient.** *J Chem Phys* 1965; 42:288–292
20. Neil JJ, Shiran SI, McKinstry RC, et al. **Normal brain in human newborns. Apparent diffusion coefficient and diffusion anisotropy measured by using diffusion tensor MR imaging.** *Radiology* 1998;209:57–66
21. Chien D, Kwong K, Gress DR, et al. **MR diffusion imaging of cerebral infarction in humans.** *AJNR Am J Neuroradiol* 1992; 13:1097–1102
22. Connelly A, Chong WK, Johnson CL, et al. **Diffusion weighted magnetic resonance imaging of compromised tissue in stroke.** *Arch Dis Child* 1997;77:38–41
23. Marks MP, De Crespigny A, Lentz D, et al. **Acute and chronic stroke. Navigated spin-echo diffusion weighted MR imaging.** *Radiology* 1996;199:403–408
24. Schlaug G, Siewert B, Benfield A, et al. **Time course of the apparent diffusion coefficient (ADC) abnormality in human stroke.** *Neurology* 1997;49:113–119
25. Baird AE, Warach S. **Magnetic resonance imaging of acute stroke.** *J Cereb Blood Flow Metab* 1998;18:583–609
26. Bruning R, Wu RH, Deimling M, et al. **Diffusion measurements in the ischemic human brain with a steady-state sequence.** *Invest Radiol* 1996;31:709–715
27. D'Arceuil HE, de Crespigny AJ, Rother J, et al. **Diffusion and perfusion magnetic resonance imaging of the evolution of hypoxic ischemic encephalopathy in the neonatal rabbit.** *J Magn Reson Imaging* 1998;8:820–828
28. Lovblad K, Jakob PM, Chien Q, et al. **Turbo spin-echo diffusion-weighted MR of ischemic stroke.** *AJNR Am J Neuroradiol* 1998; 19:201–208
29. Moseley ME, Kucharczyk J, Mintorovitch J, et al. **Diffusion-weighted MR imaging of acute stroke. Correlation with T2-weighted and magnetic susceptibility enhanced MR imaging in cats.** *AJNR Am J Neuroradiol* 1990;11:423–429
30. Ahn SS, Mantello MT, Jones KM, et al. **Rapid MR imaging of the pediatric brain using the fast spin-echo technique.** *AJNR Am J Neuroradiol* 1992;13:1169–1177
31. Barkovich AJ, Hajnal BL, Vigneron D, et al. **Prediction of neuromotor outcome in perinatal asphyxia. Evaluation of MR scoring systems.** *AJNR Am J Neuroradiol* 1998;19:143–149
32. Robertson RL, Maier SE, Robson CD, et al. **MR line scan diffusion imaging of the brain in children.** *AJNR Am J Neuroradiol* 1999;20:419–425
33. Mulkern RV, Gudbjartsson H, Westin CF, et al. **Multi-component apparent diffusion coefficients in human brain.** *NMR Biomed* 1999;12:51–62
34. Kim SG, Tsekos NV. **Perfusion imaging by a flow-sensitive alternating inversion recovery (FAIR) technique. Application to functional brain imaging.** *Magn Reson Med* 1997;37:425–435[published erratum appears in *Magn Reson Med* 1997;37::–675]
35. Vannucci RC, Christensen MA, Yager JY. **Nature, time-course, and extent of cerebral edema in perinatal hypoxic-ischemic brain damage.** *Pediatr Neurol* 1993;9:29–34
36. Lundstrom K, Pryds O, Greisen G. **Oxygen at birth and prolonged cerebral vasoconstriction in preterm infants.** *Arch Dis Child* 1995;73:81–86
37. Latour LL, Svoboda K, Mitra PP, et al. **Time-dependent diffusion of water in a biological model system.** *Proc Natl Acad Sci U S A* 1994;91:1229–1233
38. Duong TQ, Ackerman JJH, Ying HS, et al. **Evaluation of extra- and intracellular diffusion in normal and globally ischemic rat brain via 19F NMR.** *Magn Reson Med* 1998;40:1–13
39. Schaefer PW, Buonanno FS, Gonzalez RG, et al. **Diffusion-weighted imaging discriminates between cytotoxic and vasogenic edema in a patient with eclampsia.** *Stroke* 1997;28:1082–1085
40. van der Toorn A, Sykova E, Dijkhuizen RM, et al. **Dynamic changes in water ADC, energy metabolism, extracellular space volume, and tortuosity in neonatal rat brain during global ischemia.** *Magn Reson Med* 1996;36:52–60
41. Mosley ME, Cohen Y, Mintorovitch J, et al. **Early detection of regional cerebral diffusion- and T2-weighted MRI and spectroscopy.** *Mag Reson Med* 1990;14:330–346
42. Barlow CF, Domek NS, Goldberg MA, et al. **Extracellular brain space measured by S35 sulfate.** *Arch Neurol* 1961;5:102–110
43. Rumpel H, Nedelcu J, Aguzzi A, et al. **Late glial swelling after acute cerebral hypoxia-ischemia in the neonatal rat. A combined magnetic resonance and histochemical study.** *Pediatr Res* 1997;42:54–59
44. Tuor UI, Kozlowski P, Del Bigio MR, et al. **Diffusion- and T2-weighted increases in magnetic resonance images of immature brain during hypoxia-ischemia. Transient reversal posthypoxia.** *Exp Neurol* 1998;150:321–328
45. Neill JJ, Duong TQ, Ackerman JJH. **Evaluation of intracellular diffusion in normal and globally-ischemic rat brain via 133Cs NMR.** *Magn Reson Med* 1996;35:329–335
46. Norris DG, Niendorf T, Leibfritz D. **Healthy and infarcted brain tissues studied at short diffusion times. The origins of apparent restriction and the reduction in apparent diffusion coefficient.** *NMR Biomed* 1994;7:304–310
47. Martin LJ, A B, Koehler RC, et al. **Primary sensory and forebrain motor systems in the newborn brain are preferentially damaged by hypoxia-ischemia.** *J Comp Neurol* 1997;377:262–285
48. Pulera MR, Adams LM, Liu H, et al. **Apoptosis in a neonatal rat model of cerebral hypoxia-ischemia.** *Stroke* 1998;29:2622–2630
49. Hara A, Niwa M, Nakashima M, et al. **Protective effect of apoptosis-inhibitory agent, *N*-tosyl-L-phenylalanyl chloromethyl ketone against ischemia-induced hippocampal neuronal damage.** *J Cereb Blood Flow Metab* 1998;18:819–823